Petroleum and Coal, Vol. 45, 3-4, 178-183

SHEAR VISCOSITY AND DIELECTRIC PERMITTIVITY IN ASPHALT MODIFIED BY SBS

Z. Vlachovicova, J. Stastna and L. Zanzotto

Bituminous Materials Chair, Faculty of Engineering University of Calgary
2500 University Drive, Calgary, T2N 1N4, Canada

Abstract. *One regular and one polymer modified asphalt were studied in simple shear flow and in harmonic electromagnetic field. Viscosity function and complex dielectric permittivity for both asphalts were compared. The time-temperature superposition of rheological and dielectric data yields identical (or almost identical) shifting factors. A close relationship between the zero shear viscosity and conductivity of the studied asphalts was observed. In polymer modified asphalt a "pathological" behavior of viscosity function was observed. This behavior and some other effects, discussed here, points to the presence of a transient network in polymer modified asphalt.*

Key words: *asphalt, modified asphalt, viscosity, dielectric properties*

Introduction

In the search for asphalt binder with improved engineering properties, the base (conventional) asphalt is frequently blended with various polymers. Such a blending usually yields a viscoelastic material with vastly different rheological properties. Quite often the change in the material behavior of polymer modified asphalts is only weakly represented in dynamic moduli, however when studying the other material functions, these asphalts exhibit the behavior very different from the used base asphalt.

New types of binders modified by polymers or other types of materials are constantly appearing and represent a significant contribution to the road construction. Since they often bring new characteristics, outside the main domain of known materials, the testing and specifications will have to be constantly adjusted to incorporate these characteristics.

The basic thermomechanical and structural properties of viscoelastic materials are commonly studied and probed by various infinitesimal perturbations (mostly mechanical and electromagnetic).

The linear response of even very complex material systems is mathematically manageable and various experimental techniques are well developed [1,2,3].

When the perturbations of finite magnitude are applied to material systems the variety of behavior is vastly increasing and the straightforward predictions of the linear response theory do not apply.

Moreover, different experimental techniques, which for linear response yield equivalent information about the studied system, may now give different kinds of information. Thus a variety of experiments is necessary not only to improve accuracy but also to obtain information inaccessible to the linear response.

For example in mechanical response the normal stress differences which appear in the large shearing deformations of many polymeric systems represent the nonlinear response of these materials [1,4,5].

Another example of nonlinear behavior is the non-Newtonian flow observed in many polymeric systems [1,4]. The relevant material function, in this case, is the non-Newtonian viscosity function $\eta(\dot{\gamma}) = \tau_{21} / \dot{\gamma}$ (τ_{21} being the shear stress and $\dot{\gamma}$ representing the shear component of the rate of deformation tensor). The viscosity function attains the limiting value at low shear rates, i.e. the logarithmic plot of η versus $\log \dot{\gamma}$ shows a plateau which might extend over several decades of the shear rate. For larger shear rates the viscosity $\eta(\dot{\gamma})$ begins to drop and at high shear rates the logarithmic plot becomes linear, with a negative slope. The dependence of the non-Newtonian viscosity η on shear rate, at relatively low shear rates, can be associated with viscoelastic behavior in the terminal zone [1]. For example the characteristic time which determines the onset of non-Newtonian behavior with increasing shear rate is closely related to the terminal viscoelastic relaxation time [6,7,8,9]. Values of η measured at different temperatures can be reduced to a single master curve by applying the method of reduced variables [1].

When probing the material systems by electromagnetic perturbations the dielectric and conductivity measurements are frequently used [2,10]. In older methods the impedance of the tested sample is measured in conjunction with a pair of electrodes such as parallel plates. In new integrated-circuit techniques (microdielectrometry) the comb electrodes with built-in amplification and temperature sensing in a single probe are used [11,12]. Typically, the frequency range, used in these methods, is 0.01 – 10 000 Hz, However this range can be extended at both ends by various modifications of experimental methods [2]. For low frequency testing the d.c. transient current method is often employed [10]. In all dielectric measurements, the goal is to obtain the dielectric permittivity ε' and the dielectric loss factor ε''. These functions of frequency are parts of the complex dielectric permittivity (or complex dielectric constant) ε^*,

$$\varepsilon^* = \varepsilon' - i\varepsilon'' \tag{1}$$

In the absence of electrode polarization effects the complex permittivity of a material can be written as

$$\varepsilon^*(\omega) = \varepsilon'(\omega) - i(\varepsilon''(\omega) + \frac{\sigma}{\varepsilon_0 \omega}) \quad (2)$$

Here, the term $-i\sigma/\varepsilon_0\omega$ represents the d.c. contribution to the loss factor, ε_0 = 8.85e-12 F/m is the permittivity of vacuum, δ is conductivity, and is the frequency (rad/s). At low frequencies, the conductivity contribution to the loss factor is significant and may be by several orders of magnitude higher than the contribution from the dipolar relaxation. Gradually the ions and impurities in the sample may accumulate at electrodes creating a charge layer, similar to the layer of bound charge generated by dipole orientation, but with much greater charge per unit area. Then the measured capacitance (given by the total polarization charge) is much larger than the one from dipoles only. This may lead to quite large values of the apparent permittivity ε', [11].

In this contribution the shear rate dependent viscosity and the complex permittivity of a base (conventional) asphalt and its blend with the radial SBS copolymer (4%) are studied.

Experimental/Materials

The best way to improve the engineering properties of asphalt is to blend it with small amounts of selected macromolecular materials. Polymer modification causes significant changes in the stress-strain behavior of the asphalt and creates a secondary structure in the maltenic phase of asphalt. This structure then serves as a reinforcement and enhances the required properties of asphalt.

Asphalt 200/300 Pen grade was modified by 4% of SBS-radial (average molecular weight 150000, B/S ratio 70/30). The SHRP characterization of both materials is given in Table 1.

Table 1. SHRP Characterization of the Studied Asphalts

Grade	Base Asphalt 200/300	Black Max
Original Binder Properties		
Penetration @ 25°C, 100g., 5s., [dmm]	279	142
Softening Point, R&B, [°C]	35.2	61.9
Absolute Viscosity @ 60°C [Pa.s]	46.3	499.6
Kinematic Viscosity @ 135°C [mm^2/s]	190	911.8
Viscosity @ 135°C [mPa.s]	197	797.5
Dynamic Shear [G*/sin δ] [min 1.0 kPa] [kPa]	1.03	1.08
Temp [°C]	53	68
Properties after RTFOT		
RTFOT Mass Loss [%]	-0.69	-0.72
Dynamic Shear [G*/sin δ] [min 2.20 kPa] [kPa]	2.38	2.19
Temp [°C]	54	66
Properties after PAV		
PAV Aging Temperature [°C]	90	100
Dynamic Shear [G* sin δ] [max 5000 kPa] [kPa]	4412	4075
Temp [°C]	6	10
Creep stiffness [S-max. 300 MPa] @ 60s	282	280
m-value [min. 0.300] @ 60s	0.36	0.312
Temperature, [°C]	-25.9	-28
Superpave PG Grade	PG 52-34	PG 64-34
True Superpave Grade	PG53-35	PG 66-38

Radial SBS has a star structure with more than three polystyrene blocks. Polystyrene has a glass transition temperature of about 95°C, and the elastomeric blocks of rubber have a glass transition temperature of about -80°C. This difference in the glass transition temperatures of the building blocks of SBS makes this polymer very interesting for asphalt modification. Below the glass transition temperature of polystyrene a cross linked network is created. On repeated heating and cooling this crosslinking is reversible.

Samples of modified asphalt were prepared by homogenization by the high-shear mixer (170°C) and then poured into the rubberized molds. After cooling to the room temperature the samples were used for rheological testing.

Viscosity measurements were conducted at elevated temperatures (40°C to 90°C).

Rheometer used was a Rheometric Scientific ARES-33A. Testing geometry was the cone and plate with cone angle of 4° and diameter 50mm. The shear rates ranged from 5x10^{-4} to 100 [1/s].

Dielectric properties of asphalt were measured on the sample in the form of an asphalt circular disc. The actual voltage/current measurement was performed by a femtostat of the Electrochemical Impedance System EIS 900 (Gamry Instruments Inc. of Willow Grove, PA.). The asphalt sample and femtostat were in an electrostatically screened environment. The sample cell was kept in thermostatic chamber controlled by PID programmable controller (±0.1°C). The gap 0.1 mm between capacitor plates was maintained by the six ruby balls that also provided an electrical insulation of a field homogenizing ring. A special device in the form of coaxial container with a preloaded spring mechanism was used for loading the sample into the capacitor-to ensure that the prescribed gap is maintained.

Results and Discussion

The effect of blending the conventional (base) asphalt with relatively small amount (4% by weight) of radial SBS copolymer is most clearly seen when plotting the viscosity function, $\eta(\dot{\gamma})$. Figure 1 shows $\eta(\dot{\gamma})$ for the base asphalt (200/300 Pen grade) and the polymer modified asphalt (PMA, 4% SBS radial) at temperatures ranging from 40 °C to 90° C. For the lowest shear rates both asphalts attain the zero-shear viscosity, η_0. It is seen that at lower temperatures the zero-shear viscosity of PMA is much higher than that of the base asphalt. With increasing temperature this trend is preserved and for example $\eta_0(T = 70^\circ C, base) = \eta_0(T = 90^\circ C, PMA)$. The qualitative difference between $\eta(\dot{\gamma})$ for the base asphalt and the studied PMA is also seen in Figure 1 and even more in Figure 2 where $\eta(\dot{\gamma})$ of PMA is portrayed. The non-Newtonian character of $\eta(\dot{\gamma})$ in PMA is evident. Moreover the peculiar behavior of $\eta(\dot{\gamma})$ at T = 50° C, 60 °C, 70 °C is seen in Figure 2. The viscosity function starts (at low shear rates) from the zero-shear viscosity and then is decreasing with the increasing $\dot{\gamma}$. However, this decrease is not simply monotonic. The most "pathological" behavior of $\eta(\dot{\gamma})$, in the studied PMA, is seen for T 50° C. Here $\eta(\dot{\gamma})$ goes through a local maximum (after the η_0 plateau) and then decreases via a second (weak) plateau first and then monotonic decrease follows. At T=60 °C, 70° C the behavior is similar except the presence of the local maximum (right after the η_0 plateau). At even higher temperatures the presence of the second plateau is not seen (at least in the studied domain of $\dot{\gamma}$).

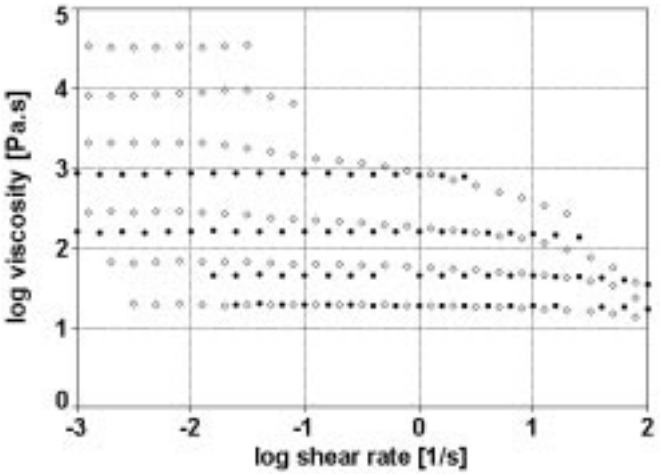

Figure 1. Viscosity of the base asphalt and PMA (4% SBS-radial).
• base asphalt, T = 40°C, 50°C, 60°C, 70°C ↓
◊ PMA, T = 40°C, 50°C, 60°C, 70°C, 80°C, 90°C ↓

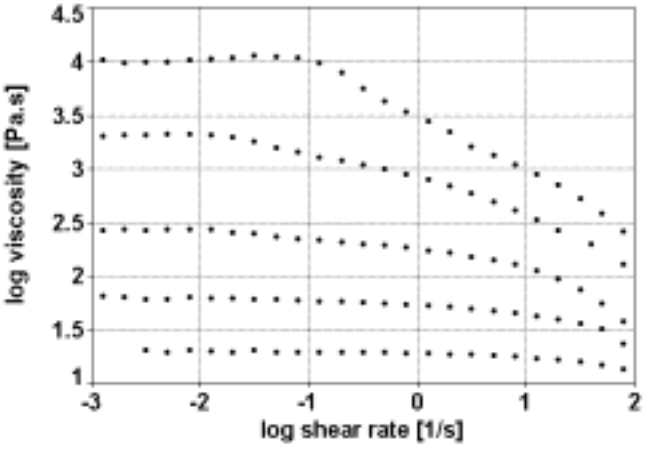

Figure 2. Viscosity of PMA (4% SBSradial); T = 50°C, 60°C, 70°C, 80°C ,90°C↓.

Dielectric properties of both asphalts are portrayed in Figures 3,4 .

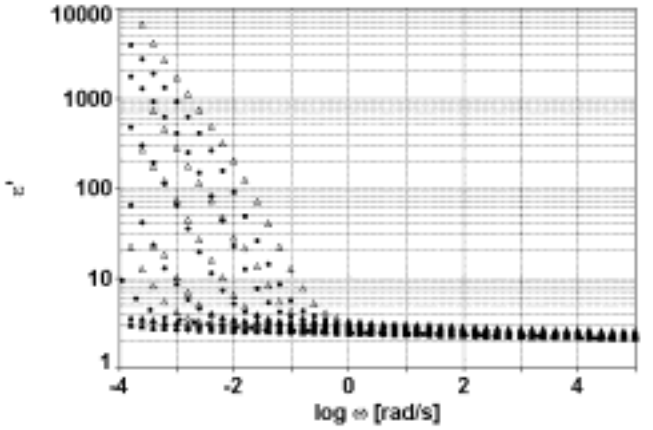

Figure 3. Dielectric permittivity(ε') of the base asphalt and PMA (4% SBS radial).
T = 0°C, 20°C, 30°C, 40°C, 48°C, 50°C, 60°C ↑; Δ base, • PMA

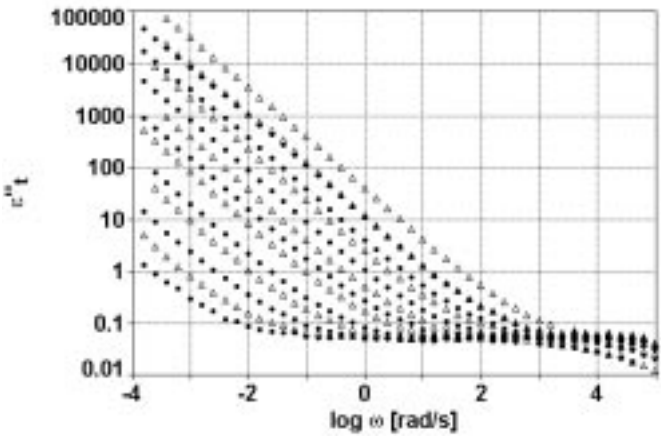

Figure 4. Dielectric loss factor (ε_t") of the base asphalt and PMA (4% SBS –radial); T = 0°C, 10°C, 20°C, 30°C, 40°C, 50°C, 60°C ↑.
Δ base, • PMA

Dielectric permittivity ε' and the "total" loss factor

$$\varepsilon_t''(\omega) = \varepsilon''(\omega) + \frac{\sigma}{\varepsilon_0 \omega} \qquad (3)$$

for temperatures ranging from 0 °C to 60 °C and frequencies between 1e-04 rad/s and 1e+05 rad/s are portrayed in these two figures. For both samples the strong conductivity contribution to the loss factor is seen in Figure 4. With increasing temperature the effect of electrode polarization is increasing and the apparent permittivity of both samples reaches very high values, Figure 3. Both conductivity and electrode polarization are higher in the base asphalt than in the studied PMA. This points to the effect of cross-linking and lesser ion (or impurities) mobility in PMA. Both components of the complex permittivity can be superposed by applying the time-temperature superposition [1]. The data of Figures 3, 4 are shifted to T = 0 °C, in Figure 5. Very small difference in dipolar relaxation can be detected by observing the part of frequency domain, $\omega \in (1, 10000)$, where the influence of conductivity is negligible and the electrode polarization is not in operation. For $\omega < 1$, the conductivity part of ε_t'' dominates the loss factor in both samples. The permittivity ε' is very slowly increasing from the value $\varepsilon' \approx 2$, at $\omega = 100000$ up to $\varepsilon' \approx 3$, at $\omega = 0.0001$. For $\omega < 0.0001$, the permittivity of both samples begins its increasing trend, due to electrode polarization, and for $\omega < 0.00001$ the increase of ε' is rapid ($\varepsilon' \approx \omega^{-\beta}$, $\beta > 0$). It is interesting to compare the horizontal shift factor, a_T , from dielectric (superposition of conductivity part of ε_t'') and mechanical (dynamic and viscosity) measurements performed on both samples. Figures 6, and 7 are such comparisons for the base and PMA samples, respectively. For the base asphalt the shift factors from mechanical and dielectric experiments are identical (taking into consideration that the experiments were performed in at least three different experimental settings), Figure 6. The comparison is not as excellent for the blend of the base asphalt and the radial SBS copolymer, see Figure 7. It is plausible that the reason for this discrepancy is the presence of cross-links in the studied PMA and the lack of cross-links in the base asphalt. It is known [1] that in polymeric systems with no cross-links the horizontal shift factor a_T is given as

$$a_T = \frac{\eta_0 T_r \rho_r}{\eta_0 T \rho} \tag{4}$$

where is the density, the zero-shear viscosity, T is the absolute temperature and subscript, *r*, refers to the reference temperature.

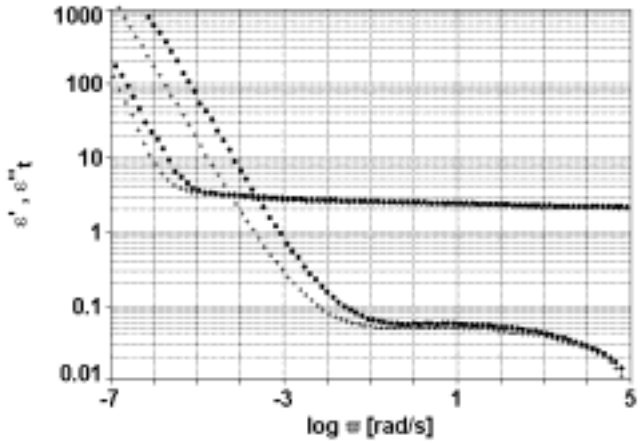

Figure 5. Dielectric permittivity (ε') and dielectric loss factor (ε_t") from figures 3,4 shifted to T = 0°C. • base; +PMA (4%SBS-radial)

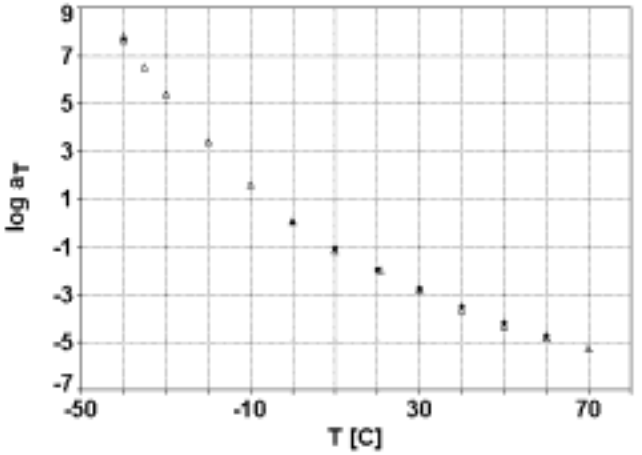

Figure 6. Horizontal time-temperature shifting factor (a_T), T_r = 0°C. Base asphalt; Δ mechanic, • dielectric

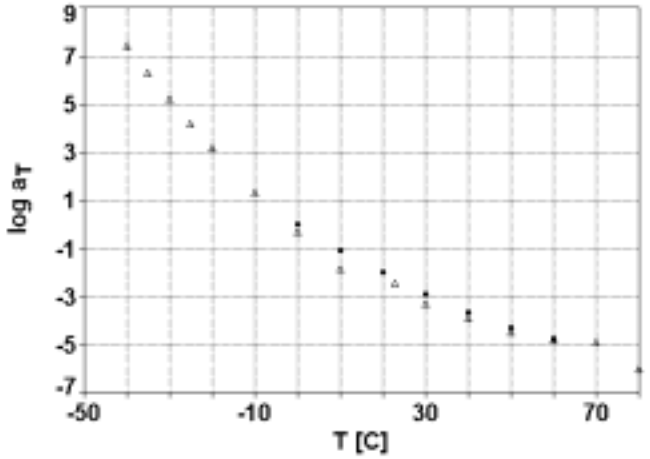

Figure 7. Horizontal time-temperature shifting factor (a_T); T_r = 0°C. PMA (4% SBS-redial); Δ mechanic, • dielectric

Then for two different temperatures T_1 and T_2 (4) yields

$$\frac{a_{T_1}}{a_{T_2}} = \frac{\eta_{01}}{\eta_{02}} \frac{T_2 \rho_2}{T_1 \rho_1} \tag{5}$$

The last relation allows to determine η_0 at various temperatures by knowing η_0 at a given temperature (the ratio ρ_2/ρ_1 is close to one). The results of such calculation, for the base asphalt, are shown in Figure 8. The similar calculation for the studied PMA was not as good as the one presented in Figure 8. Figure 9 shows another problem encountered in PMA. Here, the viscosity curves (T = 50°C, 60°C, 70° C, 80 °C, 90° C) superposed and shifted to T = 90° C are portrayed. It is clear that the "pathological" behavior of $\eta(\dot{\gamma})$ at 50 °C and 60 °C spoils the otherwise reasonable superposition.

If the parts of $\eta(\dot{\gamma})$ at T = 50 °C, 60° C are not considered the superposed curve of $\eta(\dot{\gamma})$ can be very well fitted to the Carreau-Jashuda viscosity model, [13]

$$\eta(\dot{\gamma}) = \frac{a}{\left(1 + \left(b\dot{\gamma}\right)^c\right)^{b/c}} \tag{6}$$

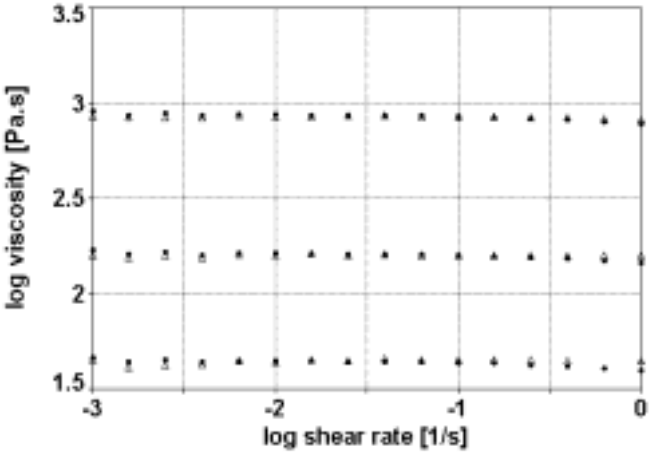

Figure 8. Viscosity at T = 40°C, 50°C, 60°C ↓ calculated from viscosity at T = 70°C. Eq. (5) with a_T from dielectric measurements. Base asphalt; Δ calculated, • experimental

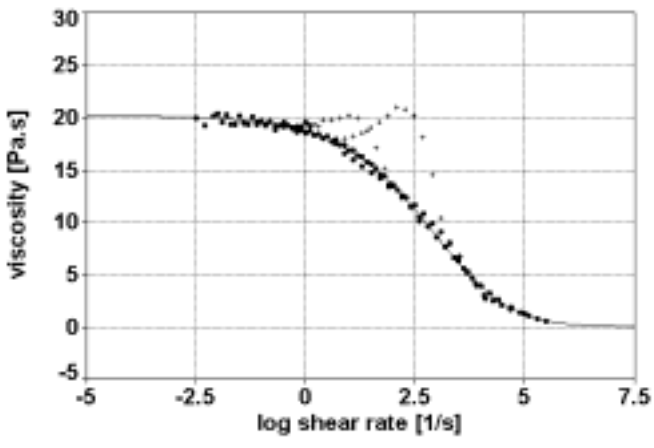

Figure 9. Viscosities of PMA (4% SBS-radial) shifted to T_r = 90°C.
• experimental, - Carreau-Jashuda fit (without +)
+ "pathological" parts of viscosities at T=50°C, 60°C

It is interesting that for the base asphalt it seems to be possible to overlap the vertically shifted part of viscosity curve and the part of the permittivity curve ($\varepsilon'(\omega)$) – the part just before the electrode polarization becomes relevant. Such a shift is shown in Figure 10, where the part of viscosity curve, at 60° C, was shifted vertically (log η_S = log η – 1.6) to the permittivity curve, at the same temperature. Here we assume that the part of ε' (log ω < 0.6) is generated by the electrode polarization , i.e. it should not be considered for the evaluation of dielectric properties of the sample. When the remaining part of ε' (log ω > 0.6) is fitted to the Davidson-Cole model [14]

$$\frac{\varepsilon^* - \varepsilon_\infty}{\varepsilon_0 - \varepsilon_\infty} = \frac{1}{(1 + i\omega\lambda)^\gamma}, 0 < \gamma < 1 \qquad (7)$$

it fits very well the curve superposed from the parts of ε' and the shifted viscosity, η_S .

The similar construction and the fit for the studied PMA are portrayed in Figure 11. Here the part of the master curve (Figure 9) of $\eta(\dot{\gamma})$ was vertically shifted and overlapped with ε' , at 50 °C. The "pathological" parts of η at 50° C and 60° C were omitted from the shifted master curve. More work is needed to fully understand the problems mentioned for the blend of the base asphalt and the small amount of radial SBS copolymer.

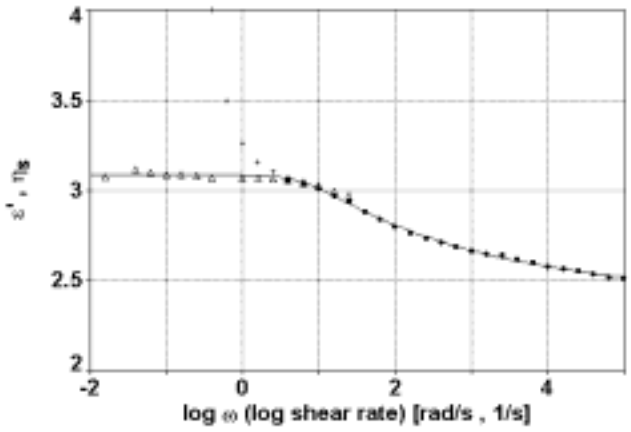

Figure 10. Superposition of dielectric permittivity and viscosity, T = 60°C. Base asphalt; • ε', Δ viscosity shifted to overlap with ε' + part of ε' corresponding to electrode polarization - Davidson-Cole model(only ε')

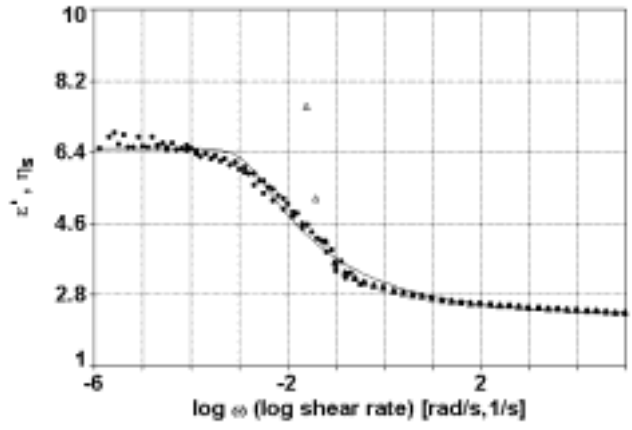

Figure 11. Master curve- viscosity and dielectric permittivity, T_r = 50°C. PMA(4% SBS-radial); • experimental Δ part of ε' corresponding to electrode polarization - Davidson-Cole model(ε' and η_S)

Relatively straightforward should be the relation between the conductivity and the zero-shear viscosity. That this is the case, for the studied asphalts, can be seen from Figures 12 and 13, where the relative conductivity (σ/σ_{40}) and the relative zero-shear viscosity ($\eta_{0_{40}}/\mu_0$), for the base asphalt and PMA, are plotted versus the absolute temperature. The reference temperature is 40° C, for both samples.

For the base asphalt the fit to simple function yields

$$\sigma(T) = \sigma_{40} K_1 \exp(-b_1 / T_2) \qquad (8)$$

and

$$\eta_0(T) = \frac{\eta_{0_{40}}}{K_1} \exp(b_1 / T^2) \qquad (9)$$

where $K_1 \doteq \exp(24.11459)$, and $b_1 \doteq 2.3684$ e+06, $[b_1] = K^2$

Similarly the fit in Figure 13 is,

$$\sigma(T) = \sigma_{40} K_2 \exp(-b_2 / T) \qquad (10)$$

and

$$\eta_0(T) = \frac{\eta_{0_{40}}}{K_2} \exp(b_2 / T) \qquad (11)$$

where $K_2 \doteq \exp(53.69)$, and $b_2 \doteq 16828.91$, $[b_2] = K$

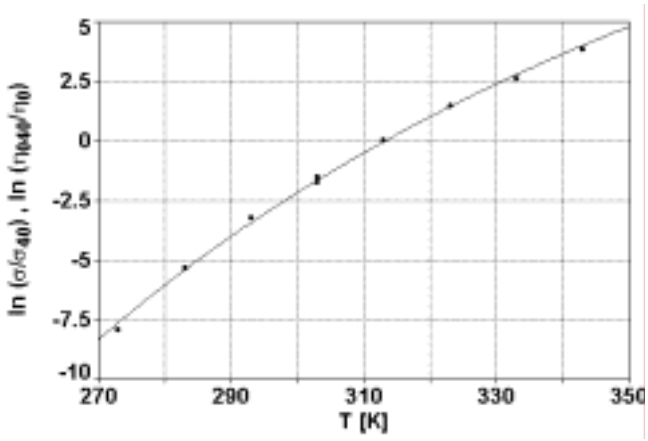

Figure 12. Relative conductivity and viscosity, T_r = 40°C. Base asphalt; • experimental, - Eqs. (8), (9).

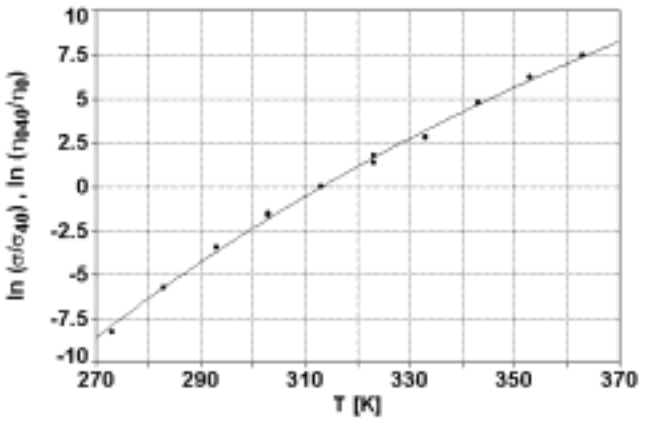

Figure 13. Relative conductivity and viscosity, T_r = 40°C. PMA (4% SBS-radial); • experimental, - Eqs. (10), (11)

Thus theoretically from the known zero-shear viscosity or the conductivity at one temperature it is possible to estimate these two quantities at an arbitrary temperature. Moreover the conductivity and the zero-shear viscosity are simply related,

$$\sigma(T)\eta_0(T) = \sigma(T_r)\eta_0(T_r) \quad (12)$$

where T_r is a reference temperature.

Finally we should stress once again the peculiar behavior of the viscosity function of polymer modified asphalts, mentioned earlier and seen in Figure 2. The double plateau and even the hint of strain hardening at temperatures around 50 °C are more or less observed in other concentrations of SBS and also in the blends of the neat asphalt with ethylene-vinyl-acetate (EVA) polymer. It was shown in [15] that the transient network model of associating polymers can predict the shear thickening at moderate shear rates followed by shear thinning at higher shear rates. This is the behavior observed also in polymer modified asphalts- at particular temperatures. We plan to investigate the use of the transient network model for the description of rheological properties of polymer modified asphalts.

Conclusions

When the base asphalt is modified by SBS copolymer the presence of an internal transient network is manifested in shear viscosity curves. Especially at T=50°C and 60°C the shear thickening followed by shear thinning was observed. With increasing temperature this behavior is changed to the regular one (plateau of the zero shear viscosity followed by monotonous decrease of the viscosity function). Dielectric properties of the studied asphalts can be shifted to a single master curve for each component of the complex dielectric permittivity. In the base asphalt the dielectric and mechanical shift factor coincide. This coincidence was observed also for the studied polymer modified asphalt, however there is a small scatter of a_T . For very low frequencies and higher temperatures the electrode polarization was observed in both studied asphalts. This polarization obscures the permittivity (ε')measurements at those regions. It is interesting that in some cases (temperatures) it is possible to shift the viscosity curve and overlap it with the permittivity curve. This shifting then can help to distinguish the "real" permittivity masked by the electrode polarization. There is clear connection between conductivity and zero shear viscosity of the studied asphalts.

Thus we hope to get better understanding of the internal structure of polymer modified asphalts by combining the rheological and dielectric observations in these materials.

Acknowledgements

The authors express their gratitude to the Natural Sciences and Engineering Research Council of Canada and to Husky Energy Ltd. for their financial support of this work.

References

[1] J. D. Ferry, Viscoelastic Proterties of Polymers, Wiley, New York (1980)
[2] N. G. McCrum, B. E. Read and G. Williams, The elastic and Dielectric Effects in Polymeric Solids (1967)
[3] K. Schmidt-Rohr and H. W. Spiess, Multidimensional Solid-State NMR and Polymers, Academic Press, London (1994)
[4] R. B. Bird, C. F. Curtiss, R. A. Armstrong and O. Hassuger, Dynamics of Polymeric Liquids 1, 2, Wiley, New York (1987)
[5] C. Truesdell and W. Noll, The Non-Linear Field Theories of Mechanics, Encyclopedia of Physics 3/3, Springer, Berlin (1965)
[6] M. Doi and S. F. Edwards, The Theory of Polymer Dynamics, Claredon Press, Oxford (1986)
[7] W. W. Graessley, The Entanglement Concept in Polymer Rheology, Adv. Polym. Sci., vol. 16, (1974)
[8] W. E. Rochefort, G. G. Smith, H. Rachapudy, V. R. Raju and W. W. Graessley, Properties of Amorphous And Crystallizable Hydrocarbon Polymers. Rheology of Linear And Star-branched Polybutadiene
[9] W. W. Graessley and L. Sega, Effect of Molecular Weight Distribution on the Shear Dependence of Viscosity in Polymer Systems, AICHE J., 16, 261-267 (1970)
[10] P. Hedvig, Dielectric Spectroscopy of Polymers, Wiley, New York (1977)
[11] D. R. Day, T. J. Lewis, H. Lee and S. D. Sentaria, The Role of Boundary Layer Capacitance at Blocking Electrodes in the Interpretation of Dielectric Cure Data in Adhesives, J. Adhesion,18,73-90 (1985)
[12] N. F. Sheppard Jr. and S. D. Sentaria, Dielectric Properties of Bisphenol-A Epoxy Resins, J. Polym. Sci. Part B: Polym. Phys., 27, 753-762 (1984)
[13] I. Sigillo and N. Grizzuti, The Effect of Molecular Weight on the Steady Shear Rheology of Lyotropic Solutions A Phenomenological Study. , J. Rheol. 38, 589-599 (1994)
[14] D. W. Davidson and R. H. Cole, Dielectric Relaxation in Glycerine, J. Chem. Phys., 18, 1471, (1950)
[15] A. Vaccaro and G. Marruci, A Model For the Nonlinear Rheology of Associating Polymers, J. Non-Newtonian Fluid Mech., 92, 261-273 (2000)